Journal of Photochemistry and Photobiology A: Chemistry 218 (2011) 111–116

Contents lists available at ScienceDirect

Journal of Photochemistry and Photobiology A: Chemistry

journal homepage: www.elsevier.com/locate/jphotochem

Effect of 2-propenyltrimethylsilane and magnetic field effect on photochemical Fe/Co fine particle formation from a ternary gaseous mixture

Hiroshi Morita [a,*], Koh Hattori [b], Jan Šubrt [c]

[a] Graduate School of Advanced Integration Science, Chiba University, Yayoi-cho, Inage-ku, Chiba 263-8522, Japan
[b] Graduate School of Science and Technology, Chiba University, Yayoi-cho, Inage-ku, Chiba 263-8522, Japan
[c] Institute of Inorganic Chemistry, Academy of Sciences of the Czech Republic, 25086 Řež near Prague, Czech Republic

ARTICLE INFO

Article history:
Received 15 October 2010
Received in revised form
28 November 2010
Accepted 8 December 2010
Available online 16 December 2010

Keywords:
Gas phase photochemical reaction
Aerosol particle
Magnetic field effect
Iron pentacarbonyl
Cobalt tricarbonyl nitrosyl
2-Propenyltrimethylsilane

ABSTRACT

From a gaseous mixture of iron pentacarbonyl ($Fe(CO)_5$), cobalt tricarbonyl nitrosyl ($Co(CO)_3NO$), and 2-propenyltrimethylsilane (allyltrimethylsilane) (ATMeSi), spherical aerosol particles with a mean diameter of 0.36 μm were produced under UV light irradiation. Addition of ATMeSi accelerated the chemical reactions of $Co(CO)_3NO$ to produce aerosol particles efficiently, and decelerated those of $Fe(CO)_5$ to inhibit the formation of crystalline deposits which were mainly composed of $Fe_2(CO)_9$ structure involving Fe–C(=O)–Co bond. Chemical structure and chemical compositions of the sedimentary aerosol particles were investigated from FT-IR and SEM–EDS analyses. Co species were rich in the sedimentary particles, and efficient excitation of $Co(CO)_3NO$ molecules at 355 nm with a Nd:YAG laser resulted in a greater abundance of Co species. Under a magnetic field of up to 5 T, sedimentary aerosol particles were synthesized from the ternary gaseous mixture. Chemical composition of the particles was dependent on magnetic field strength, and atomic ratios of Fe and Si to Co atom increased above 3 T. Magnetic field effect on the nucleation reactions was discussed briefly.

1. Introduction

In order to produce spherical particles, we have developed a photochemical method where photochemical reactions of reactive molecules initiated nucleation reactions during aerosol particle formation [1,2]. Using the photochemical method, metal containing aerosol particles were synthesized from organometal compounds such as iron pentacarbonyl ($Fe(CO)_5$) and cobalt tricarbonyl nitrosyl ($Co(CO)_3NO$) [3,4], and particle size of the sedimentary particles thus prepared was controlled by changing photochemical reaction time. In a gaseous mixture of $Fe(CO)_5$ and carbon disulfide (CS_2), particle size was reduced from 220 nm to as small as 58 nm by shortening UV irradiation time from 120 to 1 s [5]. 2-Propenyltrimethylsilane (allyltrimethylsilane) (ATMeSi) can ligate to metal atoms via π-coordination of allyl group, and can incorporate into the nucleation reaction during aerosol particle formation [6]. In a ternary gaseous mixture of $Fe(CO)_5$, CS_2, and ATMeSi, incorporation of ATMeSi molecules to the particle formation process resulted in efficient formation of long particle wires [7].

Pure $Co(CO)_3NO$ vapor produced spherical particles with a mean diameter of 80 nm under UV light irradiation, and ATMeSi vapor accelerated the chemical reactions of $Co(CO)_3NO$ molecules [8]. From a gaseous mixture of $Fe(CO)_5$ and $Co(CO)_3NO$, both the crystalline deposits and spherical aerosol particles were produced via different chemical reactions between $Fe(CO)_5$ and $Co(CO)_3NO$ [9]. In the present paper, sedimentary aerosol particles were produced from a ternary gaseous mixture of $Fe(CO)_5$, $Co(CO)_3NO$, and ATMeSi, and the role of ATMeSi on the morphology of the deposits and on the chemical reactions between $Fe(CO)_5$ and $Co(CO)_3NO$ were studied based on the analyses of FT-IR spectra and scanning electron microscopy/energy dispersive spectroscopy (SEM–EDS). Excitation efficiency of $Co(CO)_3NO$ molecules was varied by changing the excitation wavelength from 313 nm of a medium pressure mercury lamp to 355 nm of a Nd:YAG laser. Excitation wavelength dependence on chemical compositions of the sedimentary particles was analyzed by SEM–EDS. Furthermore, sedimentary aerosol particles were produced from the ternary gaseous mixture under an external magnetic field of up to 5 T. External magnetic field effects on chemical compositions of the sedimentary particles and on the nucleation reactions were discussed briefly.

2. Experimental

$Co(CO)_3NO$ (Gelest, 95%), $Fe(CO)_5$ (Kanto, 95%), and ATMeSi (Tokyo Kasei, G.R. grade) were degassed by freeze-pump-thaw cycles in the dark and purified by vacuum distillation immedi-

* Corresponding author. Tel.: +81 50 1332 5434; fax: +81 43 432 1168.
E-mail address: hmorita@faculty.chiba-u.jp (H. Morita).

1010-6030/$ – see front matter © 2010 Elsevier B.V. All rights reserved.
doi:10.1016/j.jphotochem.2010.12.010

ately before use. To prepare a gaseous mixture of $Co(CO)_3NO$, $Fe(CO)_5$, and ATMeSi, each vapor was introduced successively into a cross-shaped Pyrex cell (volume 168 cm^3) having a long (length 160 mm, inner diameter 35 mm) and short (length 80 mm, inner diameter 20 mm) arms or into a small cylindrical Pyrex cell (length 160 mm, inner diameter 20 mm, volume 50 cm^3) equipped with a couple of quartz windows through a vacuum line equipped with a capacitance manometer (Edwards Barocel Type 600). The background pressure of the irradiation cell was less than 1×10^{-4} Torr (1 Torr = 133.3 Pa). The partial pressures of $Co(CO)_3NO$, $Fe(CO)_5$, and ATMeSi in the irradiation cell were determined from the diagnostic band intensities of FT-IR spectra at 2108 cm^{-1} for $Co(CO)_3NO$, 645 cm^{-1} for $Fe(CO)_5$, and 854 cm^{-1} for ATMeSi.

The gaseous samples were irradiated with a medium pressure mercury lamp (Ushio UM-452, 450 W) through UV29 and UV-D33S filters (energy, 5.4 mJ/s cm^2) to excite both $Co(CO)_3NO$ and $Fe(CO)_5$ molecules at 365 nm and 313 nm. Light intensity at 365 nm was 1.6 times stronger than the one at 313 nm. Absorbance of 1 Torr of $Co(CO)_3NO$ and of $Fe(CO)_5$ is 0.23 and 0.06, respectively, at 365 nm, and 0.06 and 0.28, respectively, at 313 nm in 10 cm light path length. ATMeSi does not absorb any light at longer wavelengths than 220 nm. The gaseous samples were also irradiated with the third harmonic (355 nm) of pulsed Nd:YAG laser light (Continuum Surelite I-10, pulse width 6 ns, repetition rate 10 Hz) through a concave lens with a focal length of 40 or 120 mm (energy, 1.6–2.3 mJ/pulse cm^2). Absorbance of 1 Torr of $Co(CO)_3NO$ and of $Fe(CO)_5$ is 0.19 and 0.07, respectively, at 355 nm. Monitor (He–Ne laser) light intensity scattered by aerosol particles as formed in the irradiation cell during UV light irradiation was measured with a combination of a photomultiplier tube (EMI 6256S) and a lock-in amplifier (SRS SR-530) through a Y-52 filter. Both the crystalline deposits and sedimentary particles were deposited on a glass plate and/or Cu substrate placed at the bottom of the irradiation cell.

Scanning electron microscope (SEM) images were recorded with a JEOL JSM 6060 scanning electron microscope, and SEM–EDS analyses were performed using a Philips XL30 CP EDAX scanning electron microscope. FT-IR spectra of the deposits embedded in KBr pellets were measured with a Nicolet NEXUS 470 FT-IR spectrometer. Magnetic field was applied by a helium-free superconducting magnet (Toshiba TM-5SP).

3. Results and discussion

3.1. Formation of spherical aerosol particles from a ternary gaseous mixture

Under UV light irradiation with a medium pressure mercury lamp at 313 and 365 nm for 3 min, a gaseous mixture of $Fe(CO)_5$ (1.4 Torr), $Co(CO)_3NO$ (3.5 Torr), and ATMeSi (8.0 Torr) produced spherical sedimentary particles of black brown color with a mean diameter of 0.36 μm (Fig. 1(a)), whereas a binary gaseous mixture of $Fe(CO)_5$ (1.5 Torr) and $Co(CO)_3NO$ (3.2 Torr) produced crystalline deposits with sizes of ~50 μm (Fig. 1(b)) and a small amount of spherical sedimentary particles (Fig. 1(c)) under UV light irradiation for 60 min. As was reported previously [9], the binary gaseous mixture of $Fe(CO)_5$ and $Co(CO)_3NO$ produced only spherical particles without producing any crystalline deposits when a partial pressure of $Fe(CO)_5$ was decreased to lower than 0.5 Torr. By adding ATMeSi molecules which could coordinate to Fe and Co atoms via π-coordination of allyl group [7], aerosol particles were efficiently produced. However, at a lower partial pressure of ATMeSi as in a ternary gaseous mixture of $Fe(CO)_5$ (1.1 Torr), $Co(CO)_3NO$ (3.4 Torr), and ATMeSi (4.1 Torr), crystalline deposits were produced in addition to the spherical aerosol particles. A relatively high partial pressure of ATMeSi was necessary to inhibit the formation of crystalline deposits which were mainly composed of $Fe_2(CO)_9$ structure involving Fe–C(=O)–Co bond [9]. For a gaseous mixture containing 8.0 Torr of ATMeSi, monitor (He–Ne laser) light intensity scattered by aerosol particles as formed under UV light irradiation was measured; the result is shown in Fig. 2. The scattered light was detected in 5 s immediately after UV light irradiation started, and lasted over the whole period for 60 min. Rapid formation of aerosol particles is characteristic of particle formation containing organometal compounds [5,7,9]. In this experiment, UV light was turned off after 60 min. The detected scattered light disappeared in 3 min, showing that the convection period of the formed aerosol particles was about 3 min.

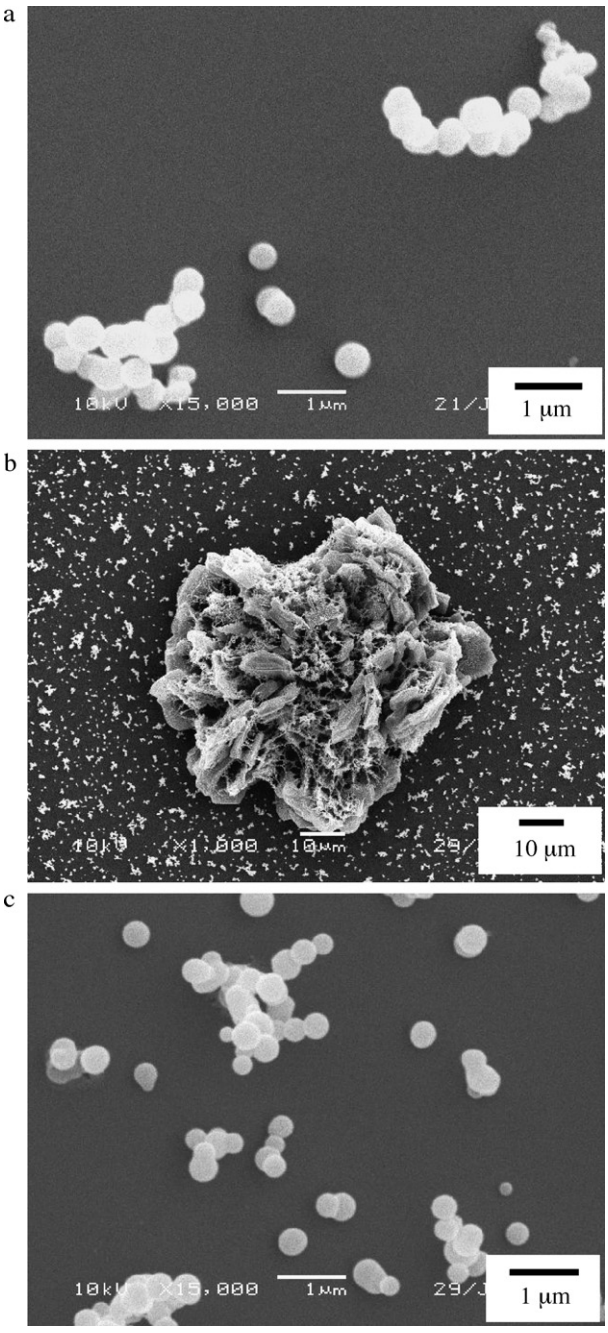

Fig. 1. SEM images of deposits produced from a gaseous mixture of (a) $Fe(CO)_5$ (1.4 Torr), $Co(CO)_3NO$ (3.5 Torr), and ATMeSi (8.0 Torr), and (b) and (c) $Fe(CO)_5$ (1.5 Torr) and $Co(CO)_3NO$ (3.2 Torr) under light irradiation for (a) 3, (b) 60, and (c) 60 min. Original magnification of SEM, (a) 15,000×, (b) 1000×, and (c) 15,000×.

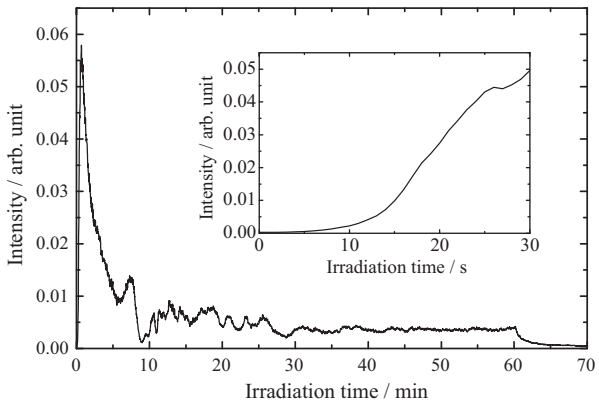

Fig. 2. He–Ne laser light intensity scattered by aerosol particles produced from a gaseous mixture of $Fe(CO)_5$ (1.4 Torr), $Co(CO)_3NO$ (3.5 Torr), and ATMeSi (8.0 Torr) under light irradiation with a medium pressure mercury lamp.

FT-IR spectrum of the sedimentary particles produced from the ternary gaseous mixture under UV light irradiation for 3 min is shown in Fig. 3. The spectrum was very similar to the one of the sedimentary particles produced from a binary gaseous mixture of $Fe(CO)_5$ and $Co(CO)_3NO$ except that weak bands assignable to $\delta(Si–(CH_3)_3)$ of ATMeSi were observed at 1250 and 841 cm^{-1}. This indicated that ATMeSi was incorporated into the particle formation process without changing the chemical interaction between $Fe(CO)_5$ and $Co(CO)_3NO$.

Chemical composition of the sedimentary aerosol particles was studied by SEM–EDS analysis. Under the present experimental conditions, Cu substrate was covered partly with sedimentary particles. Hence, Cu signal which came from uncovered substrate was eliminated during the analysis. Furthermore, the results of SEM–EDS were slightly dependent on the measuring spots on the Cu substrate, suggesting that the sample may not be homogeneous. In the present analysis, the results at several measuring spots were averaged. The population of Fe, Co, Si, C, N, and O atoms was 9.7, 16.6, 1.5, 22.9, 5.7, and 43.5 at%, respectively. Some fraction of the O and also of the C (and N) signals could originate from oxidation of the Cu substrate and the surface contamination with hydrocarbons present prior to particle deposition [10]. Thus, except for C, N, and O atoms, atomic ratios among Fe, Co, and Si atoms were reliable in the analysis. Atomic ratio of Fe to Co atom was 0.58 (1:1.7) (with an experimental uncertainty of 0.04 due to sample inhomogeneity), revealing that the particles were more rich in Co species than Fe species. ATMeSi was incorporated into the particles in a ratio of 0.09 ∓ 0.02 to Co species. In the sedimentary particles produced from a binary gaseous mixture of $Fe(CO)_5$ and $Co(CO)_3NO$, atomic ratio of Fe to Co atom was 0.68–0.91 depending on initial partial pressures of the samples [9]. By the addition of ATMeSi, Co species were more abundant in the sedimentary particles.

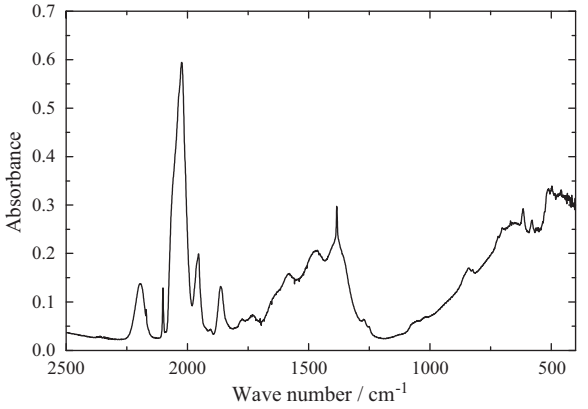

Fig. 3. FT-IR spectrum of sedimentary aerosol particles produced from a gaseous mixture of $Fe(CO)_5$ (1.4 Torr), $Co(CO)_3NO$ (3.5 Torr), and ATMeSi (8.0 Torr) under light irradiation with a medium pressure mercury lamp for 3 min.

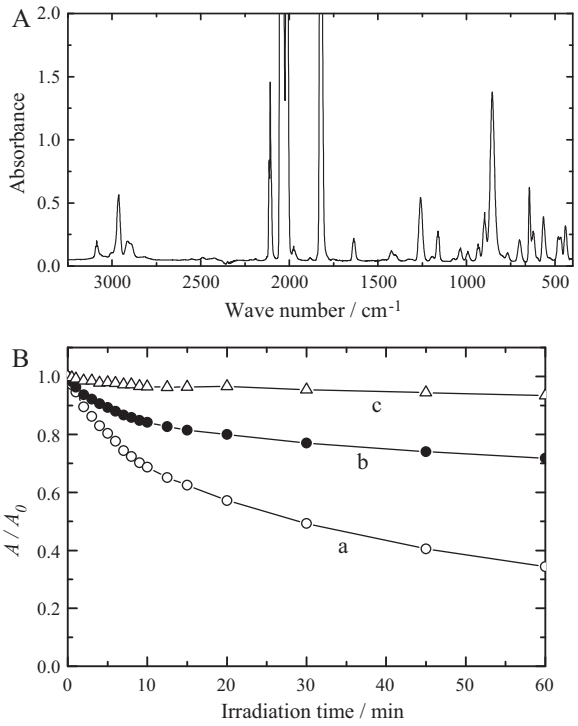

Fig. 4. (A) FT-IR spectrum of a gaseous mixture of $Fe(CO)_5$ (1.4 Torr), $Co(CO)_3NO$ (3.5 Torr), and ATMeSi (8.0 Torr), and (B) depletion (A/A_0) of (a) δ(Fe–C–O) band at 645 cm^{-1} of $Fe(CO)_5$, (b) ν(C≡O) band at 2108 cm^{-1} of $Co(CO)_3NO$, and (c) $\delta(Si–(CH_3)_3)$ band at 854 cm^{-1} of ATMeSi against irradiation time.

Chemical processes in the gas phase were investigated by measuring FT-IR spectrum of a gaseous mixture of $Fe(CO)_5$ (1.4 Torr), $Co(CO)_3NO$ (3.5 Torr), and ATMeSi (8.0 Torr). The spectrum of the gaseous mixture is shown in Fig. 4(A). Upon UV light exposure, FT-IR bands of $Fe(CO)_5$, $Co(CO)_3NO$, and ATMeSi decreased their intensities. After allowing for complete sedimentation of the formed aerosol particles, the band intensity (absorbance, A) of δ(Fe–C–O) band at 645 cm^{-1} of $Fe(CO)_5$ [11–13], of ν(C≡O) band at 2108 cm^{-1} of $Co(CO)_3NO$ [14,15], and of $\delta(Si–(CH_3)_3)$ band at 854 cm^{-1} of ATMeSi [16,17] was measured, and the ratio of A to the initial absorbance before light irradiation, A_0, was plotted against cumulative irradiation time (Fig. 4(B)). In the ternary gaseous mixture, $Fe(CO)_5$, $Co(CO)_3NO$, and ATMeSi molecules were consumed by ~65%, ~28%, and 6%, respectively, after 60 min under UV light irradiation. The number of molecules depleted from the gaseous phase was estimated to be 0.15, 0.21,and 0.10 Torr, respectively, over 3 min under UV light irradiation. The molar ratio of depleted $Fe(CO)_5$ to depleted $Co(CO)_3NO$ molecules was 1:1.4, which was close to the value (1:1.7) analyzed by SEM–EDS. Assuming the pseudo first order decay, the depletion rates of $Fe(CO)_5$, $Co(CO)_3NO$, and ATMeSi were estimated. The results are tabulated in Table 1. Compared to the corresponding values of binary gaseous mixture of $Fe(CO)_5$ and $Co(CO)_3NO$ [9], depletion rate of $Fe(CO)_5$ was decelerated by 50%, and that of $Co(CO)_3NO$ was accelerated by 20%, due to the presence of ATMeSi, showing that ATMeSi molecules were incorporated into the nucleation reaction to inhibit the formation of crystalline deposits which were mainly composed of $Fe_2(CO)_9$ structure involving Fe–C(=O)–Co bond. In a binary gaseous mixture of $Co(CO)_3NO$ and ATMeSi, the depletion rate of $Co(CO)_3NO$ was accelerated by five times due to the presence of ATMeSi [8]. ATMeSi contributed to efficient formation of aerosol particles.

Table 1
Depletion rates (in $10^{-4}\,s^{-1}$) of $Fe(CO)_5$, $Co(CO)_3NO$, and ATMeSi in pure vapor (2 Torr), in a binary gaseous mixture of $Fe(CO)_5$ (0.4 Torr) and $Co(CO)_3NO$ (2.4 Torr), and in a ternary gaseous mixture of $Fe(CO)_5$ (1.4 Torr), $Co(CO)_3NO$ (3.5 Torr), and ATMeSi (8.0 Torr) under light irradiation with a medium pressure mercury lamp.

	Gaseous sample		
	Pure vapor	Binary mixture	Ternary mixture
$Fe(CO)_5$	62	19	8.7
$Co(CO)_3NO$	3.0	4.1	5.0
ATMeSi	–	–	0.72

Under UV light irradiation, $Fe(CO)_5$ and $Co(CO)_3NO$ evolve CO and/or NO groups to produce reactive species (reactions (1)–(3)) [18–20].

$$Fe(CO)_5 + h\nu \rightarrow Fe(CO)_4 + CO \quad (1)$$

$$Co(CO)_3NO + h\nu \rightarrow Co(CO)_3 + NO \quad (2)$$

$$Co(CO)_3NO + h\nu \rightarrow Co(CO)_2NO + CO \quad (3)$$

As discussed previously [9], the nucleation reaction of particle formation from a gaseous mixture of $Fe(CO)_5$ and $Co(CO)_3NO$ proceeds via any reactive dicobalt species such as $Co_2(CO)_6NO$ (reaction (4)). These dicobalt species react with $Fe(CO)_5$ and/or $Fe(CO)_4$ to form chemical species involving Co and Fe atoms (reaction (5)).

$$Co(CO)_3 + Co(CO)_3NO \rightarrow Co_2(CO)_6NO \quad (4)$$

$$Co_2(CO)_6NO + Fe(CO)_5 \quad \text{and/or} \quad Fe(CO)_4 \rightarrow \text{Chemical species involving Co and Fe atoms} \quad (5)$$

Co atoms can be connected directly or via a bridging >C=O group as in the structure of $Co_2(CO)_8$ [21–24]. Weakening of the IR band of the bridging >C=O group and appearance of the bands in 1250–1650 cm^{-1} region ascribed to C–O bond coordinated to a metal atom strongly suggest that (1) Fe atom in $Fe(CO)_4$ which is produced from $Fe(CO)_5$ via photodecomposition [18,19] coordinates the O atom in Co–C(=O)–Co structure to form Co–C–O–Fe structure and to result in the shift of the C–O stretching vibrational frequency to 1250–1650 cm^{-1} region, and/or (2) under UV light irradiation, two CO groups in such chemical species as $Co_2(CO)_6NO$ (reaction (4)) form α-diketone structure, and the O atoms in the diketone structure coordinate to Fe atom in $Fe(CO)_4$ to show the ν(CO) band at 1500–1530 cm^{-1} [25].

During the particle formation, ATMeSi ligates to Fe and/or Co atoms via π-coordination of allyl group [12].

$$Fe(CO)_4 + CH_2{=}CH{-}CH_2{-}Si(CH_3)_3 \rightarrow (Fe(CO)_3{\cdot}CH_2{=}CH{-}CH_2{-}Si(CH_3)_3) + CO \quad (6)$$

$$Co(CO)_3 + CH_2{=}CH{-}CH_2{-}Si(CH_3)_3 \rightarrow (Co(CO)_2{\cdot}CH_2{=}CH{-}CH_2{-}Si(CH_3)_3) + CO \quad (7)$$

Fe and Co complexes with π-coordinated ATMeSi may react with $Co_2(CO)_6NO$ to produce spherical particles (reactions (8) and (9)).

$$Co_2(CO)_6NO + (Fe(CO)_3{\cdot}CH_2{=}CH{-}CH_2{-}Si(CH_3)_3) \rightarrow \text{Chemical species involving Co, Fe, and Si atoms} \quad (8)$$

$$Co_2(CO)_6NO + (Co(CO)_2{\cdot}CH_2{=}CH{-}CH_2{-}Si(CH_3)_3) \rightarrow \text{Chemical species involving multi nuclear Co atoms} \quad (9)$$

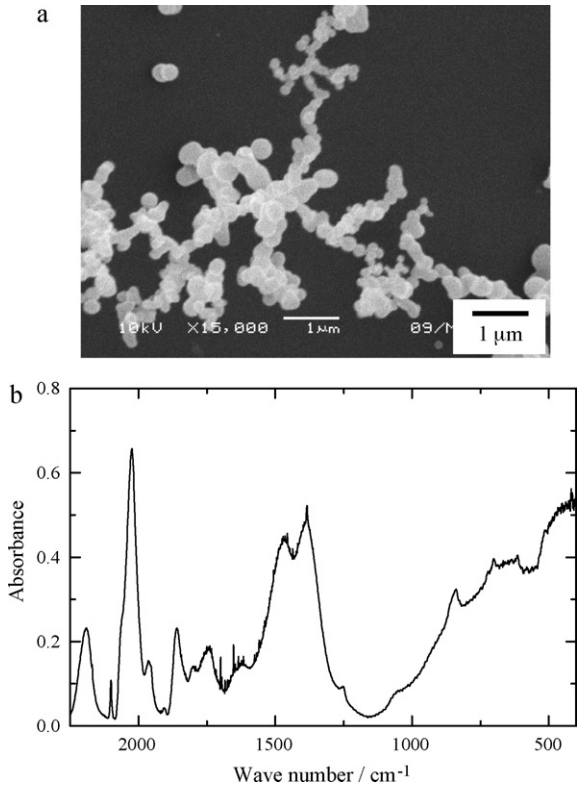

Fig. 5. (a) SEM image and (b) FT-IR spectrum of sedimentary aerosol particles produced from a gaseous mixture of $Fe(CO)_5$ (0.5 Torr), $Co(CO)_3NO$ (2.8 Torr), and ATMeSi (9.7 Torr) under light irradiation with a Nd:YAG laser at 355 nm for 3 min. Original magnification of SEM, 15,000×.

Considering that ATMeSi decelerated the depletion of $Fe(CO)_5$ in the gaseous phase, reaction (6) competed with chemical reaction to form the crystalline deposits which were mainly composed of $Fe_2(CO)_9$ structure (reactions (10)).

$$Fe(CO)_4 + Fe(CO)_5 \rightarrow Fe_2(CO)_9 \quad (10)$$

In the crystalline deposits, any chemical species involving Fe and Co atoms may be formed via chemical reaction between $Co(CO)_3$ and $Fe_2(CO)_9$ (reaction (11)).

$$Co(CO)_3 + Fe_2(CO)_9 \rightarrow \text{Chemical species involving Co and Fe atoms (such as } Fe_2Co(CO)_{12}) \quad (11)$$

Through π-coordination of ATMeSi to Fe and Co atoms, reactions (10) and (11), hence the formation of the crystalline deposits was suppressed in the ternary gaseous mixture.

3.2. Aerosol particle formation under light irradiation with a Nd:YAG laser

$Co(CO)_3NO$ molecules absorb 355 nm light more efficiently than $Fe(CO)_5$ molecules. Absorbance of 1 Torr of $Co(CO)_3NO$ and $Fe(CO)_5$ molecules is 0.19 and 0.07, respectively, in 10 cm light path length. Upon light exposure with a Nd:YAG laser, narrow laser beam was expanded through a concave lens with a focal length of 40 mm (energy 1.6 mJ/pulse cm^2) in order to irradiate entire volume of an irradiation cell. From a ternary gaseous mixture of $Fe(CO)_5$ (0.5 Torr), $Co(CO)_3NO$ (2.8 Torr), and ATMeSi (9.7 Torr), spherical particles with a mean diameter of 0.26 μm were produced under light irradiation at 355 nm for 3 min. SEM image and FT-IR spectrum of the spherical particles are shown in Fig. 5. Compared to the

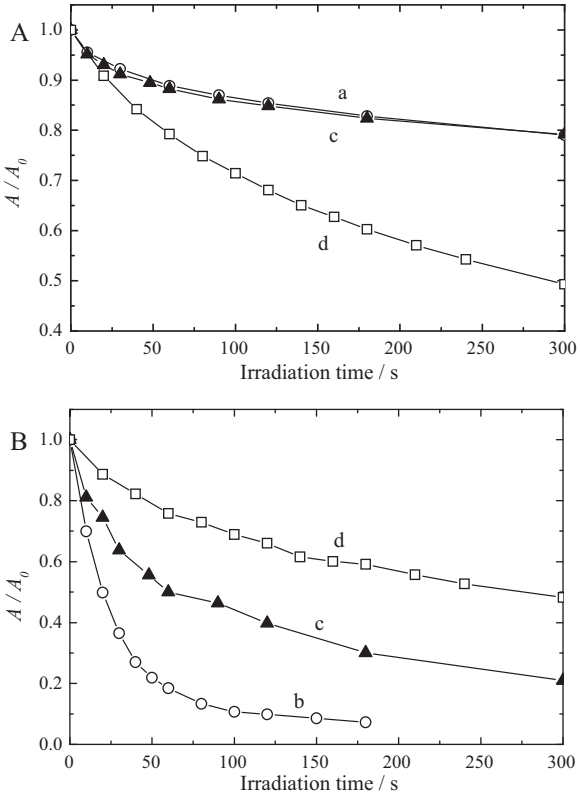

Fig. 6. Depletion (A/A_0) of (A) ν(C≡O) band at 2108 cm^{-1} of $Co(CO)_3NO$ and (B) δ(Fe–C–O) band at 645 cm^{-1} of $Fe(CO)_5$ against irradiation time in (a) pure $Co(CO)_3NO$ vapor (3.2 Torr), (b) pure $Fe(CO)_5$ vapor (0.5 Torr), and in a gaseous mixture of (c) $Fe(CO)_5$ (0.5 Torr) and $Co(CO)_3NO$ (2.9 Torr) and (d) $Fe(CO)_5$ (0.5 Torr), $Co(CO)_3NO$ (2.8 Torr), and ATMeSi (9.7 Torr).

spectrum of the particles deposited under light irradiation with a medium pressure mercury lamp (Fig. 3), band intensities of bridging ν(C=O) bands at 1860, 1799, and 1739 cm^{-1} and of 1250 and 841 cm^{-1} bands ascribed to trimethylsilyl group became stronger, indicating that chemical species having bridging C=O group such as in Co–C(=O)–Co structure became abundant and ATMeSi molecules were involved in a greater amount in the particles. SEM–EDS analysis showed that atomic ratio of Co to Fe atom was 7.2:1 for the particles deposited under light irradiation with a YAG laser. The value was larger than the one (1.7:1) of the particles produced under light irradiation with a medium pressure mercury lamp. Efficient excitation of $Co(CO)_3NO$ molecules favored the chemical reactions (4), (5), (7), and (9) to result in a greater abundance of Co species in the particles.

In order to determine the depletion rates of $Co(CO)_3NO$ and $Fe(CO)_5$ molecules, FT-IR band intensities (A/A_0) of ν(C≡O) band at 2108 cm^{-1} of $Co(CO)_3NO$ and of δ(Fe–C–O) band at 645 cm^{-1} of $Fe(CO)_5$ were plotted against cumulative irradiation time for a binary gaseous mixture of $Fe(CO)_5$ (0.5 Torr) and $Co(CO)_3NO$ (2.9 Torr) and for a ternary gaseous mixture of $Fe(CO)_5$ (0.5 Torr), $Co(CO)_3NO$ (2.8 Torr), and ATMeSi (9.7 Torr), compared to those of pure vapors (Fig. 6). Assuming the pseudo first order decay, the depletion rates of $Fe(CO)_5$ and $Co(CO)_3NO$ molecules were evaluated; the results are tabulated in Table 2. Compared the values in the ternary gaseous mixture to those in the binary gaseous mixture, depletion rate of $Fe(CO)_5$ was decelerated to one-third, and that of $Co(CO)_3NO$ was accelerated by 25%, due to the presence of ATMeSi, showing that the formation of crystalline deposits of $Fe_2(CO)_9$ (reaction (10)) was inhibited by π-coordination of ATMeSi molecules via reaction (6), and π-coordinated ($Co(CO)_2$·ATMeSi) complex was incorporated into the particle formation process via

Table 2
Depletion rates (in 10^{-3} s^{-1}) of $Fe(CO)_5$, $Co(CO)_3NO$, and ATMeSi in pure vapor ($Fe(CO)_5$ 0.6 Torr, $Co(CO)_3NO$ 3.2 Torr), in a binary gaseous mixture of $Fe(CO)_5$ (0.5 Torr) and $Co(CO)_3NO$ (2.9 Torr), and in a ternary gaseous mixture of $Fe(CO)_5$ (0.5 Torr), $Co(CO)_3NO$ (2.8 Torr), and ATMeSi (9.7 Torr) under light irradiation with a Nd:YAG laser at 355 nm.

	Gaseous sample		
	Pure vapor	Binary mixture	Ternary mixture
$Fe(CO)_5$	34	16	4.9
$Co(CO)_3NO$	2.6	3.3	4.2
ATMeSi	–	–	0.25

reaction (9). Due to efficient absorption of 355 nm light, depletion rates of $Fe(CO)_5$ and $Co(CO)_3NO$ were faster than the corresponding values under light irradiation with a medium pressure mercury lamp.

3.3. Magnetic field effect on chemical compositions of spherical particles

Chemical compositions of aerosol particles produced from a binary gaseous mixture of $Fe(CO)_5$ and $Co(CO)_3NO$ were influenced by the application of a magnetic field as reported previously [9]. From a ternary gaseous mixture of $Fe(CO)_5$ (0.4 Torr), $Co(CO)_3NO$ (3.2 Torr), and ATMeSi (8.8 Torr), spherical particles were produced in a superconducting magnet under light irradiation with a Nd:YAG laser at 355 nm for 5 min using a cylindrical cell with an inner diameter of 20 mm. In this experiment, laser beam was expanded using a concave lens with a focal length of 120 mm (energy 1.8–2.3 mJ/pulse cm^2). Magnetic field effects on the chemical structure and chemical compositions of the sedimentary aerosol particles were investigated from FT-IR and SEM–EDS analyses. FT-IR spectra of the sedimentary particles produced under a magnetic field of 0–5 T are shown in Fig. 7(A). Compared to absorbance of the 1389 cm^{-1} band of Co complex assignable to bridging >C=O bond coordinated to a metal atom, absorbance of the 2026 cm^{-1} band of terminal C–O group of Fe complex and of the 841 cm^{-1} band assigned to trimethylsilyl group was plotted against magnetic field strength in Fig. 7(B). Normalized absorbance of the 2026 cm^{-1} band of terminal C–O group of Fe complex decreased until 1 T, and then increased up to 5 T, whereas the 841 cm^{-1} band of trimethylsilyl group slightly increased its normalized absorbance above 3 T. Atomic ratios of Fe, Co, and Si atoms analyzed by SEM–EDS are tabulated in Table 3. Considering the sample may not be homogeneous, the results which were analyzed at several measuring spots were averaged, resulting in an experimental uncertainty of 0.02 in the ratios. The results in Table 3 showed that Co species were rich in the particles, and with increasing magnetic field above 3 T, atomic ratios of Fe to Co atom and of Si to Co atom increased, supporting the results from FT-IR spectra. Magnetic field dependence of the normalized absorbance of Fe species strongly suggested that abundance of Co species increased at 1 T, whereas Fe species became more abundant above 3 T. This may lead to the suggestion that chemical reaction (9) resulting in more abundance of Co species was accelerated at low

Table 3
Atomic ratios of Fe and Si to Co atom in sedimentary particles produced from a gaseous mixture of $Fe(CO)_5$ (0.4 Torr), $Co(CO)_3NO$ (3.2 Torr), and ATMeSi (8.8 Torr) under light irradiation with a Nd:YAG laser at 355 nm for 5 min in the presence of a magnetic field of 0, 1, 3, and 5 T.

	Magnetic field			
	0 T	1 T	3 T	5 T
Fe	0.29	0.29	0.34	0.31
Co	1	1	1	1
Si	0.16	0.15	0.22	0.21

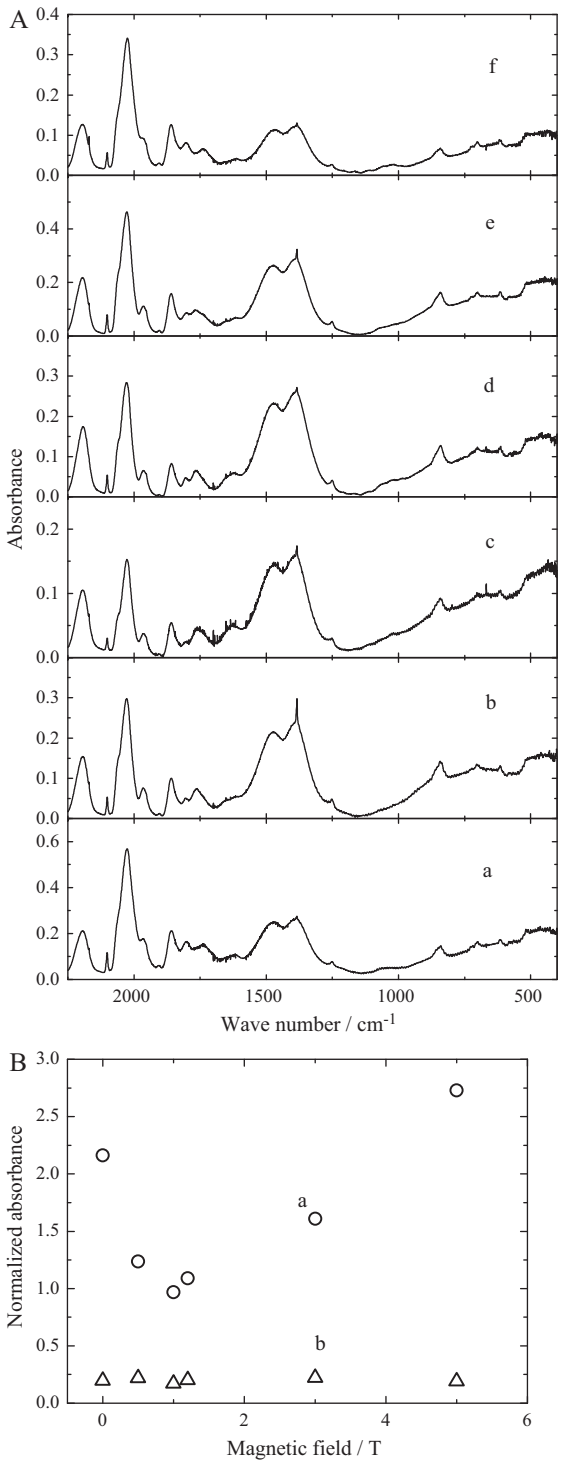

Fig. 7. (A) FT-IR spectra of sedimentary aerosol particles produced from a gaseous mixture of $Fe(CO)_5$ (0.4 Torr), $Co(CO)_3NO$ (3.2 Torr), and ATMeSi (8.8 Torr) under light irradiation with a Nd:YAG laser at 355 nm for 5 min in the presence of a magnetic field of (a) 0, (b) 0.5, (c) 1, (d) 1.2, (e) 3, and (f) 5 T. (B) Absorbance of (a) 2026 cm^{-1} band and (b) 841 cm^{-1} band normalized to absorbance of 1389 cm^{-1} band as a function of magnetic field.

magnetic field and chemical reactions (5) and (8) resulting in more abundance of Fe species were accelerated at higher magnetic field. From a similarity to the magnetic field dependence frequently observed in geminate radical pairs in solutions and micelles [26–29], acceleration of chemical reaction (9) may be saturated at low magnetic field near 1 T, whereas chemical reactions (5) and (8) were accelerated in a greater degree with increasing magnetic field. It is noteworthy that intensity change of the IR band ascribed to terminal C–O group was accompanied by the change in chemical structure of C–O group. Hence, the intensity change of the IR band may be larger than the change in atomic ratio of Fe to Co atom. The increase of atomic ratio of Fe to Co atom under a magnetic field was also observed during aerosol particle formation from a binary gaseous mixture of $Fe(CO)_5$ and $Co(CO)_3NO$ [9]. This supported that the nucleation reactions of the ternary gaseous mixture were essentially the same to those of the binary gaseous mixture.

During aerosol particle formation, several chemical reactions take place concurrently. Among these reactions, some are accelerated or decelerated by the application of a magnetic field. Although a mechanism to induce any change in the reaction rate has not yet been clarified [10], magnetic field induces a change in chemical structure and chemical composition of the particles. Thus, a magnetic field can be utilized to control the chemical properties of the sedimentary particles.

4. Conclusions

From the ternary gaseous mixture of $Fe(CO)_5$, $Co(CO)_3NO$, and ATMeSi, spherical aerosol particles were efficiently produced under UV light irradiation. Addition of ATMeSi accelerated the chemical reactions of $Co(CO)_3NO$ to produce aerosol particles efficiently, and decelerated those of $Fe(CO)_5$ to inhibit the formation of crystalline deposits which were mainly composed of $Fe_2(CO)_9$ structure involving Fe–C(=O)–Co bond. Co species were rich in the sedimentary particles, and efficient excitation of $Co(CO)_3NO$ molecules at 355 nm with a Nd:YAG laser resulted in a greater abundance of Co species. Chemical structure and chemical composition of the particles were influenced by the application of a magnetic field. With increasing magnetic field above 3 T, atomic ratios of Fe to Co atom and of Si to Co atom increased. From a detailed analysis of the magnetic field effect on chemical structure, it was suggested that the nucleation reactions involving Fe species responded to the magnetic field differently from those involving Co species.

References

[1] H. Morita, J. Photopolym. Sci. Technol. 12 (1999) 95.
[2] H. Morita, J. Photopolym. Sci. Technol. 21 (2008) 767.
[3] H. Morita, Y. Takeyasu, H. Okamura, H. Ishikawa, Sci. Technol. Adv. Mater. 7 (2006) 389.
[4] K. Abe, H. Morita, J. Photopolym. Sci. Technol. 19 (2006) 135.
[5] H. Morita, Y. Takeyasu, J. Šubrt, J. Photochem. Photobiol. A 197 (2008) 88.
[6] H. Morita, H. Ishikura, J. Photopolym. Sci. Technol. 18 (2005) 193.
[7] H. Morita, K. Abe, M. Takahashi, J. Photochem. Photobiol. A 210 (2010) 108.
[8] H. Morita, H. Sakano, C. Yamano, J. Photopolym. Sci. Technol. 20 (2007) 117.
[9] H. Morita, A. Kasai, J. Šubrt, Z. Bastl, J. Photochem. Photobiol. A 206 (2009) 205.
[10] H. Morita, R. Nozawa, Z. Bastl, Mol. Phys. 104 (2006) 1711.
[11] M. Bigorgne, J. Organomet. Chem. 24 (1970) 211.
[12] L.H. Jones, R.S. McDowell, M. Goldblatt, B.I. Swanson, J. Chem. Phys. 57 (1972) 2050.
[13] R.K. Sheline, K.S. Pitzer, J. Am. Chem. Soc. 72 (1950) 1107.
[14] G. Bor, J. Organomet. Chem. 10 (1967) 343.
[15] L.H. Jones, R.S. McDowell, B.I. Swanson, J. Chem. Phys. 58 (1973) 3757.
[16] J.R. Durig, J.F. Sullivan, A.W. Cox Jr., B.J. Streusand, Spectrochim. Acta A 34 (1978) 719.
[17] V.S. Nikitin, M.V. Polyakova, I.I. Baburina, A.V. Belyakov, E.T. Bogoradovskii, V.S. Zavgorodnii, Spectrochim. Acta A 46 (1990) 1669.
[18] M. Poliakoff, J.J. Turner, J. Chem. Soc. Dalton Trans. (1973) 1351.
[19] M. Poliakoff, E. Weitz, Acc. Chem. Res. 20 (1987) 408.
[20] W. Wang, F. Chen, J. Lin, Y. She, J. Chem. Soc. Faraday Trans. 91 (1995) 847.
[21] G.G. Sumner, H.P. Klug, L.E. Alexander, Acta Crystalogr. 17 (1964) 732.
[22] R.L. Sweany, T.L. Brown, Inorg. Chem. 16 (1977) 415.
[23] D.L. Lichtenberger, T.L. Brown, Inorg. Chem. 17 (1978) 1381.
[24] J.P. Kenny, R.B. King, H.F. Schaefer III, Inorg. Chem. 40 (2001) 900.
[25] K. Babić-Samardžija, S.P. Sovilj, N. Katsaros, J. Mol. Struct. 694 (2004) 165.
[26] Y. Tanimoto, H. Hayashi, S. Nagakura, H. Sakuragi, K. Tokumaru, Chem. Phys. Lett. 41 (1976) 267.
[27] Y. Sakaguchi, H. Hayashi, S. Nagakura, J. Phys. Chem. 86 (1982) 3177.
[28] H. Hayashi, S. Nagakura, Bull. Chem. Soc. Jpn. 57 (1984) 322.
[29] H. Hayashi, Y. Sakaguchi, M. Wakasa, Bull. Chem. Soc. Jpn. 74 (2001) 773.